

# Wind and Air Temperature Distributions in the Wake of a Running Vehicle

Takeshi Sato, Kenji Kosugi, Osamu Abe, Shigeto Mochizuki and Sanji Koseki

Snow and Ice Research Group

National Research Institute for Earth Science and Disaster Prevention  
Tokamachi, Shinjo, Yamagata 996-0091, Japan

Tel: +81-233-22-7550, Fax: +81-233-22-7554, E-mail: tsato@bosai.go.jp

## Abstract

The snow and ice melt or refreeze through natural heat exchange and they are also subject to the mechanical and thermal effects of running vehicles. This study focuses on the turbulent heat transfer in the wake of a running vehicle. For the first step of its estimation, we observed the wind and air temperature distributions in the wake, air temperatures around the running vehicle, and exhaust pipe temperature.

The wind speed in the wake decreased with distance from the rear end of the vehicle and increased with vehicle speed. The turbulence characteristics had a similar tendency. Applying the surface layer theory to the wind field in the wake, we found the turbulent momentum transfer in the wake to be enhanced. The heating of air in the wake due to the running vehicle extended up to about 20 m from the rear end. The temperature of the exhaust pipe depended not only on the vehicle speed but also on the inclination of the road, since the engine revolution changes accordingly. The heating of air, defined by the air temperature difference between ‘front’ and ‘end’, depended on the vehicle speed, inclination of the road, and atmospheric stability on the road.

## 1. Introduction

The state of snow and ice on roads influences the safety of traffic in winter. Snow and ice melt or refreeze through heat exchange whose components are short- and long-wave radiations, sensible and latent heats under windy conditions, and heat conduction to/from the roadbed. This situation is identical to that in the case of natural snow cover. In addition, on roads, snow and ice are subject to the mechanical effects of running vehicles, and vehicles generate heat. The heat is transferred to the snow and ice by heat conduction from tires (e.g., Kinoshita *et al.*, 1970; Takeshi *et al.*, 2002), thermal radiation (e.g., Ishikawa *et al.*, 2000), and turbulence generated by the vehicle itself.

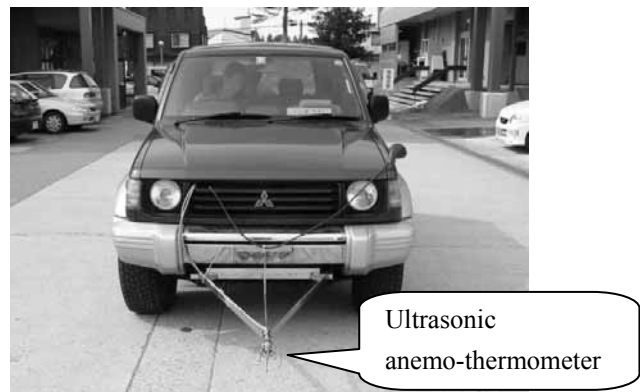


Fig. 1 The wind and air temperature sensor attached to the observing vehicle in OBS-A.

The present study focuses on this turbulent heat transfer. Turbulence behind a vehicle has been studied from the viewpoint of air pollutant diffusion (e.g., Eskridge and Hunt, 1979), but it is not known whether the turbulent heat transfer to the road surface is effective, and no method for estimating it has been established.

As the first step to answering these questions, we observed the wind and air temperature distributions in the wake formed behind a running vehicle (OBS-A), and observed the air temperatures around a running vehicle and the exhaust pipe temperature (OBS-B).

## 2. Method

### 2.1. Wind and air temperature distributions in the wake (OBS-A)

A vehicle drove at a constant speed, 40 or 60 km/h, and an observing vehicle followed it at the same speed, keeping a constant distance. An ultrasonic anemo-thermometer attached to the observing vehicle measured the three components of wind speed and air temperature at a frequency of up to 10 Hz (Fig. 1). The sensor height was 50 cm above the ground surface. The distance to the vehicle in front was measured with a laser range finder.

The wind speed observed from a coordinate system fixed to space is given by

$$\vec{V} = \vec{V}_m + \vec{V}_c, \quad (1)$$

where  $\vec{V}_m$  is the measured wind speed and  $\vec{V}_c$  is the vehicle speed. This observation was carried out on a straight flat road under calm conditions. If the observed wind and air temperature are stationary, their spatial distributions are considered to move at the same speed as the vehicle speed.

### 2.2. Air temperatures around the vehicle (OBS-B)

The temperature sensors to measure the air temperature around the vehicle were attached to the tips of the bars fixed to the front and rear fenders, and attached above the roof (Fig. 2). The front and roof sensors measured the air temperatures that were not thermally affected by the vehicle. Three sensors at the rear measured the air temperatures heated by the vehicle. Another temperature sensor was attached to the hottest part exposed to the underfloor airflow, namely the surface of the exhaust pipe.

The position of the vehicle was recorded every two seconds using GPS, from which the vehicle speed was calculated. This observation was carried out on two routes; one was a flat route, where the road was dry, and another was an uphill and downhill route, where there were some tunnels and the road was wet or covered with slush or compacted snow.



Fig. 2 The air temperature sensors attached to the vehicle in OBS-B.

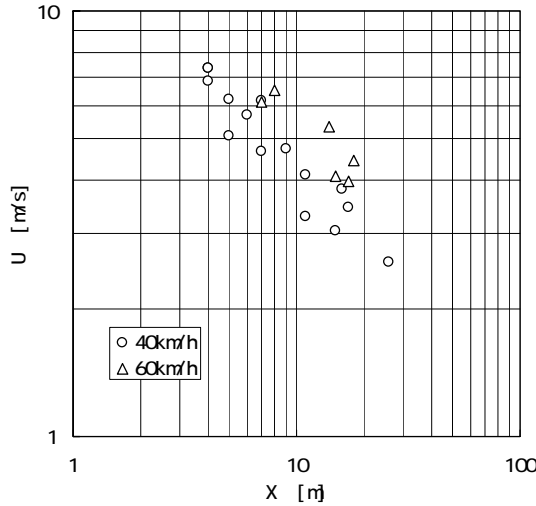


Fig. 3 The relationship between the wind speed and the distance from the rear end of the running vehicle.

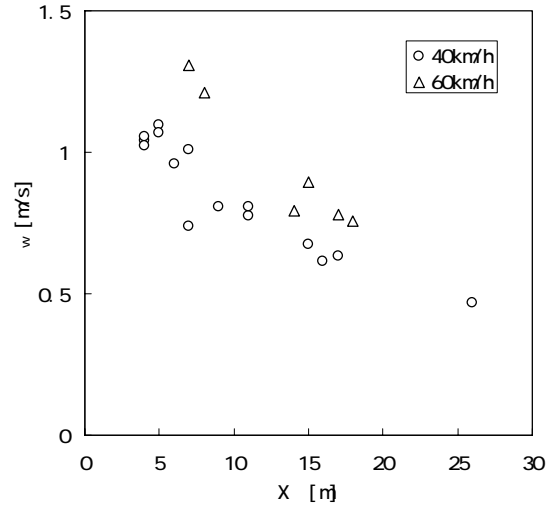


Fig.4 The relationship between the standard deviation of the vertical component of fluctuating wind and the distance from the rear end of the running vehicle.

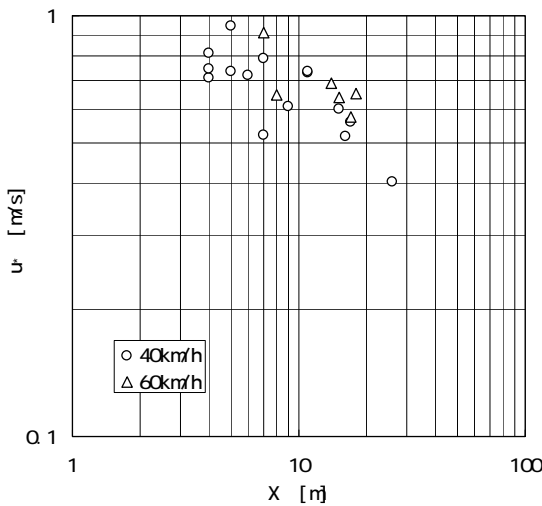


Fig.5 The relationship between the friction velocity and the distance from the rear end of the running vehicle.

### 2.3. Selection of data

In OBS-A, the data satisfying constant vehicle speed were selected. In OBS-B, the data were selected, which satisfied a vehicle speed of more than 40 km/h and the gentle change of road steepness in order to avoid rapid changes of running conditions. The data in the tunnel were not analyzed for OBS-B.

## 3. Results and discussion

### 3.1. Wind and air temperature distributions in the wake (OBS-A)

Figure 3 shows the distribution of wind speed,  $U$ , in the wake, which is a component in the running direction and is defined with reference to the coordinate system fixed to space. The different

symbols correspond to the vehicle speed. The wind speed decreases with the distance from the rear end of the vehicle,  $X$ , and increases with the vehicle speed. The relationship is expressed by

$$U \propto U_c^{2/3} X^{-1/2}, \quad (2)$$

where  $U_c$  is the vehicle speed. Since  $U_c$  has only two values, the dependence on  $U_c$  is tentative. If the wake is characterized by the wind speed distribution, it extends more as the vehicle speed becomes high.

Figures 4 and 5 show the distributions of the characteristics of turbulence in the wake. The standard deviation of the vertical component of fluctuating wind (Fig. 4) decreases with distance and increases with vehicle speed. The friction velocity,  $u^*$ , showed a similar tendency (Fig. 5);  $u^*$  is

proportional to  $X^{-1/3}$ . The rate of decrease of  $u_*$  with  $X$  is smaller than that of the wind speed.

The turbulent transfer in the wake is discussed on the basis of these measurements. For reference, the surface layer on a homogeneous plain is considered, where the turbulent diffusivity is usually expressed by

$$K = ku_*z \quad (3)$$

Here,  $k$  is the von Karman constant and  $z$  is the height. The logarithmic wind speed profile is derived from Eq. (3) as

$$U(z) = \frac{u_*}{k} \ln \frac{z}{z_0} \quad (4)$$

where  $z_0$  is the roughness length, which is a constant corresponding to the roughness of the surface.

If the logarithmic law is assumed to hold for the height interval from 0 to 50 cm in the wake, the apparent roughness length,  $z_{0,e}$  (hereafter, the effective roughness length) can be obtained from the following equation:

$$U(z) = \frac{u_*}{k} \ln \frac{z}{z_{0,e}} \quad (5)$$

The effective roughness length is plotted in Fig. 6 against the distance from the rear end of the vehicle. The effective roughness length is not constant and it increases with the distance.

In the wake, generated turbulence is constrained by the solid wall and its nature is partly affected by the ground surface. In other words, the wall turbulence is affected by the eddy in the wake, and the turbulent transfer is modified from that of the pure wall turbulence. Therefore, a factor,  $\alpha$ , is introduced to account for this. The turbulent diffusivity is assumed in the following way:

$$K = \alpha ku_*z \quad (6)$$

If  $\alpha = 1$ , the turbulent transfer has the same efficiency as in the surface layer over a homogeneous

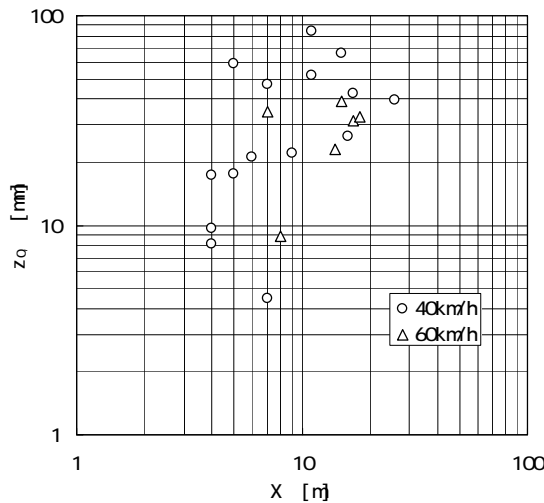


Fig.6 The relationship between the effective roughness length and the distance from the rear end of the running vehicle.

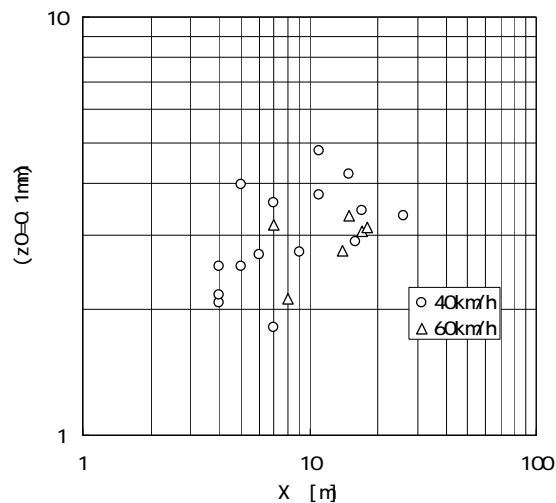


Fig. 7 The relationship between  $\alpha$  and the distance from the rear end of the running vehicle.

plain. If  $\alpha > 1$ , the turbulent transfer is more efficient than in the surface layer over a homogeneous plain. The wind profile, similar to Eq. (4), is derived from Eq. (6) as

$$U(z) = \frac{u_*}{\alpha k} \ln \frac{z}{z_0} \quad (7)$$

The value of  $\alpha$  can be obtained by using Eqs. (5) and (7) if  $z = 500$  mm, and  $z_0 = 0.1$  mm is assumed. The  $\alpha$ -value increases with the distance from the rear end of a running vehicle, as shown in Fig. 7. This means that the eddy in the wake evolves downstream, enhancing the turbulent transfer in the wake compared to that in the surface layer over a homogeneous plain.

Next, the air temperature distribution in the wake is shown in Fig. 8, where the ordinate is the air temperature difference between inside the wake and outside the wake. The temperature difference is large if the distance from the rear end is short, and it decreases with distance. At a distance of more than about 20 m, the temperature difference is close to zero, showing that the hot air is almost diffused.

### 3.2. Air temperatures around the vehicle (OBS-B)

An example of the air temperatures around the running vehicle and the exhaust pipe temperature is shown in Fig. 9 together with the altitude and vehicle speed. The route was first uphill and then downhill. The vehicle drove at almost constant speed. The exhaust pipe temperature

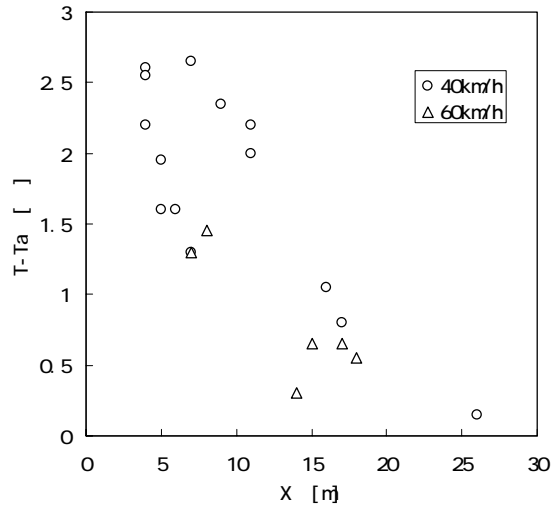


Fig. 8 The relationship between the air temperature difference between inside the wake and outside the wake and the distance from the rear end of the running vehicle.

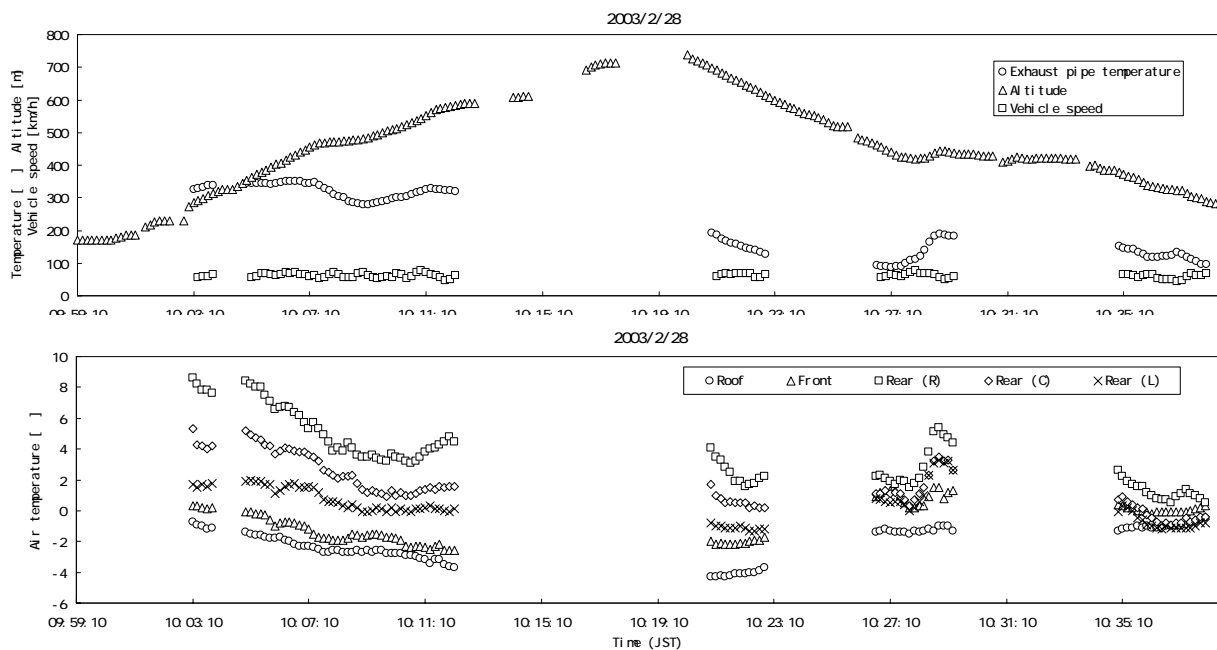


Fig. 9 Time series of the exhaust pipe temperature, altitude, and vehicle speed (upper), and air temperatures around the running vehicle (lower).

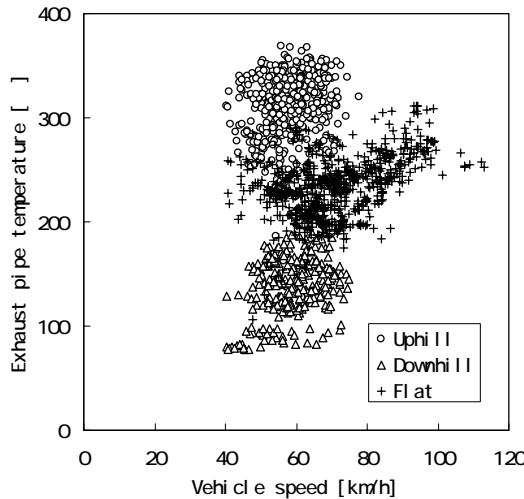


Fig.10 The relationship between the exhaust pipe temperature and the vehicle speed.

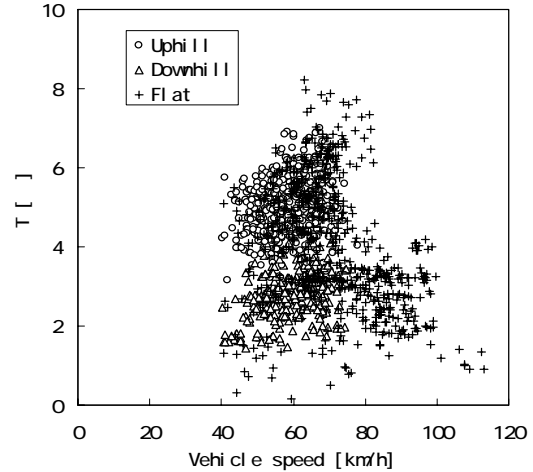


Fig.11 The relationship between the air temperature difference,  $\Delta T$  ('rear'-'front'), and the vehicle speed.

was higher on the uphill route and lower on the downhill route. The lower figure shows the air temperatures around the running vehicle.

The exhaust pipe temperature is plotted in Fig. 10 against the vehicle speed. The temperature increases with the vehicle speed, which can be seen in the flat case. The temperatures are clearly classified according to the inclination of the road. This can be ascribed to the difference in the engine revolution that depends on the inclination even at the same vehicle speed.

The air temperature difference,  $\Delta T = \text{'rear' - 'front'}$ , where 'rear' is an average of three air temperatures, 'rear(L)', 'rear(C)', and 'rear(R)', is plotted in Fig. 11 against the vehicle speed. The  $\Delta T$ -value corresponds to the amount of heating by the vehicle. In the uphill and downhill cases, the temperature difference increases with the vehicle speed.  $\Delta T$  is larger in the uphill case than in the downhill case. However, in the case of the flat route, the points are scattered and there is no significant relationship.

To find the reason for this scattering,  $\Delta T$  satisfying the vehicle speed range from 55 to 65 km/h are plotted in Fig. 12 against another air temperature difference,  $\delta T = \text{'roof' - 'front'}$ . Because  $\delta T$  is actually the vertical temperature difference of the undisturbed air, it can be used as an index of the atmospheric stability on the road. If it is negative (positive), the atmosphere is unstable (stable). The measurements on the flat route are distributed over a wide range of stabilities. The stability dependence is approximated by the solid line. The  $\Delta T$ -value for the stability range of uphill and

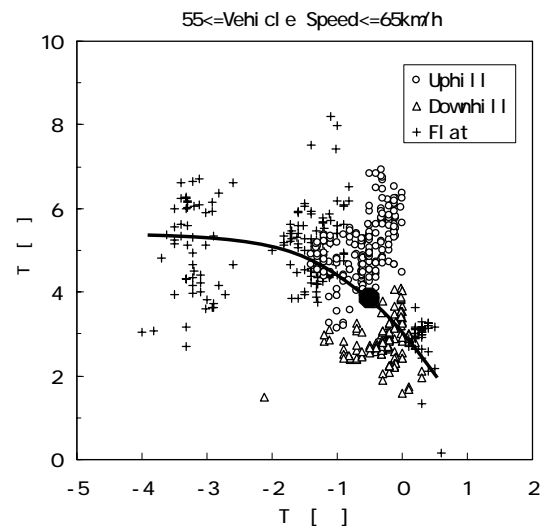


Fig.12 The relationship between the air temperature differences,  $\Delta T$  ('rear'-'front') and  $\delta T$  ('roof'-'front'). Details are shown in the text.

downhill cases, which is shown by the solid circle, lies between the values for the uphill and downhill cases. The order of the  $\Delta T$ -value coincides with that of the exhaust pipe temperature.

#### **4. Concluding remarks**

Our results show that the turbulent momentum transfer is enhanced by the eddy in the wake of a running vehicle. We clarified the amount and the distribution of heating of air due to the running vehicle, and its dependence on the vehicle speed, the inclination of road, and atmospheric stability. It remains for us to evaluate the turbulent heat transfer to the snow and ice on roads from running vehicles.

#### **References**

- Eskridge, R. E. and Hunt, J. C. R., 1979: Highway modeling. Part I: Prediction of velocity and turbulence fields in the wake of vehicles. *J. Appl. Meteorol.*, **8**, 387–400.
- Ishikawa, N., Narita, H. and Kajiya, Y., 2000: Heat balance characteristics of snow melting on roads. *Proceedings of 2000 Cold Region Technology Conference*, 383–388 (in Japanese).
- Kinosita, S, Akitaya, E. and Tanuma, K., 1970: Snow and ice on roads II. *Low Temp. Sci., Ser. A*, **28**, 311–323 (in Japanese with English summary).
- Takeshi, T., Fukuhara, T., Yokoyama, T., Watanabe, H., Hayashi, K. and Fujimoto, A., 2002: A numerical model for road icing estimation used by heat energy balance method: Heat transfer between tyre, compacted snow layer and road surface. *Proceedings of 2002 Cold Region Technology Conference*, 71–76 (in Japanese).